J. Fluid Mech. (2002), *vol.* 472, *pp.* 373–397.
DOI: 10.1017/S0022112002002434 Printed in the United Kingdom

Impact of a drop onto a wetted wall: description of crown formation and propagation

By I. V. ROISMAN AND C. TROPEA

Chair of Fluid Mechanics and Aerodynamics, Technical University of Darmstadt
Petersenstr. 30, 64287 Darmstadt, Germany

(Received 31 October 2001 and in revised form 1 July 2002)

The impact of a drop onto a liquid film with a relatively high impact velocity, leading to the formation of a crown-like ejection, is studied theoretically. The motion of a kinematic discontinuity in the liquid film on the wall due to the drop impact, the formation of the upward jet at this kinematic discontinuity and its elevation are analysed. Four main regions of the drop and film are considered: the perturbed liquid film on the wall inside the crown, the unperturbed liquid film on the wall outside the crown, the upward jet forming a crown, and the free rim bounding this jet. The theory of Yarin & Weiss (1995) for the propagation of the kinematic discontinuity is generalized here for the case of arbitrary velocity vectors in the inner and outer liquid films on the wall. Next, the mass, momentum balance and Bernoulli equations at the base of the crown are considered in order to obtain the velocity and the thickness of the jet on the wall. Furthermore, the dynamic equations of motion of the crown are developed in the Lagrangian form. An analytical solution for the crown shape is obtained in the asymptotic case of such high impact velocities that the surface tension and the viscosity effects can be neglected in comparison to inertial effects. The edge of the crown is described by the motion of a rim, formed due to the surface tension.

Three different cases of impact are considered: normal axisymmetric impact of a single drop, oblique impact of a single drop, and impact and interaction of two drops. The theoretical predictions of the height of the crown in the axisymmetric case are compared with experiments. The agreement is quite good in spite of the fact that no adjustable parameters are used.

1. Introduction

The recent progress in the field of drop and spray impact on a wetted wall can be attributed to rapid development of experimental techniques, allowing one to obtain high-quality images of impacting drops and to collect detailed information about the splashing threshold (Walzel 1980; Mundo, Sommerfeld & Tropea 1994; Wang & Chen 2000), drop shape, crown propagation, fingering of the rim, etc. (Levin & Hobbs 1971; Macklin & Metaxas 1976; Cossali, Coghe & Marengo 1997; Cossali *et al.* 1999), as well as to measure distributions of the secondary drops in the impinging spray using the phase Doppler technique (Mundo, Sommerfeld & Tropea 1998; Roisman *et al.* 1999) or using a photocamera (Shin & McMahon 1990). Several reviews (Rein 1993; Prosperetti & Oguz 1993) can be recommended for further details of the phenomena.

Detailed data, including the velocity field in the drop and film, can also be obtained using a direct numerical simulation of the drop impact (Harlow & Shannon 1967; Schelkle *et al.* 1999; Weiss & Yarin 1999) or even of multiple drop impacts (Böhm,

Weiss & Tropea 1999). These data can be especially important at the initial stages of the drop impact, at times of order of $t_1 = D_0/U_0$, when the geometry of the droplet is complicated and the theoretical analysis of the problem provides only order of magnitude values and not exact solutions. Here D_0 and U_0 are the initial droplet diameter and impact velocity, respectively. However, experiments show that the duration of the crown evolution is usually much larger than t_1. Moreover, at large times after the impact, the radius of the crown is much larger than the thickness of the crown or the thickness of the film on the wall. Therefore, the computations of the drop impact require a fine mesh and a large computation domain and are very time consuming. On the other hand, the small thickness of the crown and the film on the wall at large times, $t \gg t_1$, makes the phenomena very attractive for theoretical modelling. This modelling is possible as a remote asymptote at distances much larger than D_0.

In the theoretical work of Yarin & Weiss (1995) the impact of a drop onto a liquid film is considered. The crown-like jet formed by the impact is described in their work as a kinematic discontinuity of the liquid film. The velocity fields in the liquid film on the wall and the expansion of the base of the crown in the axisymmetric case of a normal drop impact were expressed analytically. Following their theory, the base of the crown can be considered as a kinematic discontinuity of radius R_B, subdividing the liquid film on the wall into two parts: an outer unperturbed film of constant film thickness h_f and radial velocity $V_f = 0$; and an inner part of thickness h_l and radial velocity V_l, where at large times

$$\overline{V}_l(\bar{r}, \bar{t}) = \frac{\bar{r}}{\bar{t} + \bar{\tau}}, \quad \bar{h}_l(\bar{r}, \bar{t}) = \frac{\bar{\eta}}{(\bar{t} + \bar{\tau})^2}, \quad \overline{R}_B(\bar{t}) = \bar{\beta}\,(\bar{t} + \bar{\tau})^{1/2}. \tag{1.1 a–c}$$

Here the overbar denotes a dimensionless value with the drop initial diameter D_0 used as a length scale and its impact velocity U_0 as a velocity scale. The radial coordinate is denoted r, and the time since initial impact is denoted t. Parameters $\bar{\beta}$, $\bar{\tau}$ and $\bar{\eta}$ are dimensionless constants depending on the parameters of the impact: Reynolds number, Weber number and the dimensionless initial film thickness $\bar{h}_f$. Equation (1.1) satisfies the mass and momentum balance in the film on the wall and the jump conditions at the kinematic discontinuity.

The expression (1.1c) for the radius of the base of the crown agrees well with the experimental data of Yarin & Weiss (1995) and Cossali *et al.* (1999). Moreover, the predictions of this radius by (1.1c) describe very accurately the results obtained by Rieber & Frohn (1999) using the three-dimensional volume-of-fluid numerical method of solution of the Navier–Stokes equations.

In the recent work of Trujillo & Lee (2001) the theory of Yarin & Weiss (1995) for the propagation of the kinematic discontinuity is generalized to take into account the effect of the viscous forces. The model improves the results of prediction of the propagation of the radius of the crown. However, the differences with the theory of Yarin & Weiss are not large. This indicates that in the case of high impact velocities the main influencing factor on the formation of the crown is the inertia of the liquid.

In the study of polydisperse spray impingement (Tropea & Roisman 2000) it has been shown that the resulting flux of splashed droplets is not a simple superposition of single-drop impact events arising from the primary droplets of the impacting spray. One of the reasons for this is the interaction of neighbouring crowns. Such a situation is shown in figure 1. In this image, taken using a high-speed camera, the impact of a polydisperse water spray onto the north pole of a steel spherical target is shown. Two neighbouring splashing crowns can be clearly seen, as well as a drop impacting in

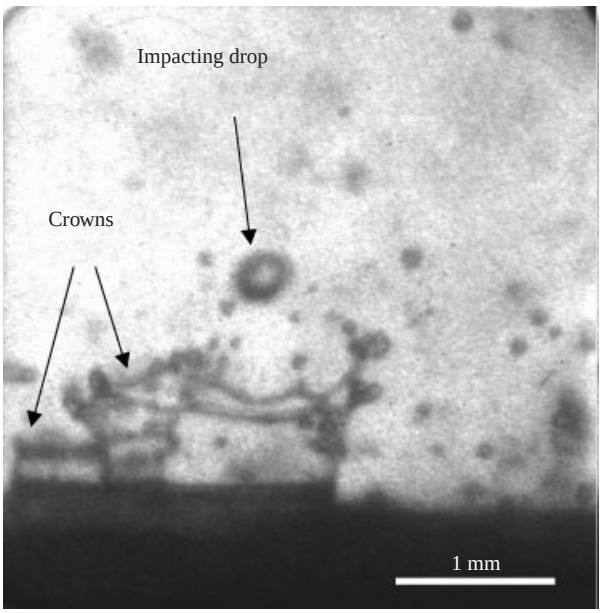

FIGURE 1. Crowns formed due to polydisperse spray impact onto a rigid wall and their interactions. Image taken using a high-speed camera.

the same region. The parameter characterizing the probability of crown interactions at the wall depends on the number flux of the impacting drops, the rate of change of the crown diameter and the total time of the crown propagation. This lifetime of the crown is determined by the motion of the rim: its initial elevation and its descent due to surface tension and gravity. The instant when the rim falls onto the wall corresponds to the total time of the crown propagation, and is one of the key parameters for modelling a dense polydisperese spray impact.

The main subject of the present work is the description of the expansion of a crown ejected from the wetted wall due to impact of a liquid drop. The impacting drop and the crown are shown schematically in figure 2. Four main regions are considered: the liquid film on the wall inside the crown (region 1 in figure 2), the undisturbed film on the wall outside the crown (region 2), the jet (region 3), and the free rim bounding the crown from above (region 4).

The crown is ejected from the boundary between regions 1 and 2, a kinematic discontinuity, where the film thickness and the velocity of the liquid both jump. The radius vectors $\boldsymbol{X}_B$, $\boldsymbol{X}_J$ and $\boldsymbol{X}_R$ (see figure 2) correspond to the front of the kinematic discontinuity, to the wall of the crown and to the centreline of the free rim, respectively.

The crown is formed due to impact with a relatively high initial drop velocity U_0. Thus, in these cases, the Reynolds number $Re = U_0 D_0/\nu$ and the Weber number $We = \rho D_0 U_0^2/\sigma$ are much larger than unity; ν, ρ and σ are the constant kinematic viscosity, density, and surface tension of the liquid respectively. Moreover, the Reynolds number $Re_h = U_0 h_f/\nu$ based on the thickness h_f of the undisturbed film is also assumed to be large. Therefore, the phenomenon of the crown formation and propagation is assumed to be inertia dominated and viscosity effects are neglected in the present analysis.

Note however, that even at these high values of We, Re and Re_h the velocity

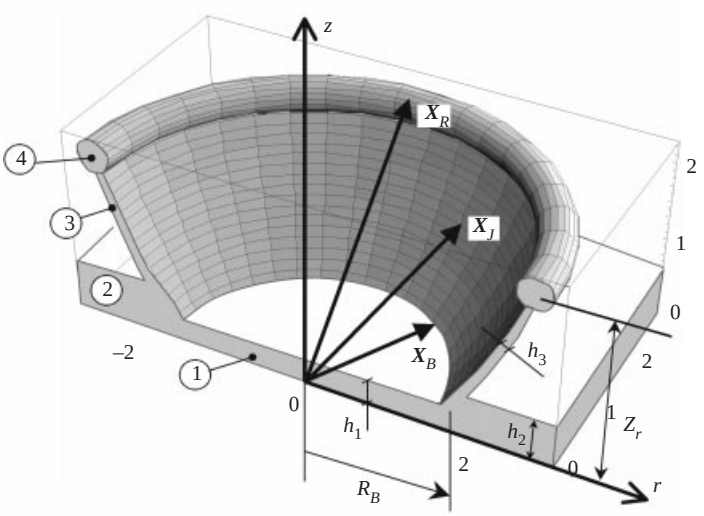

FIGURE 2. Sketch of the crown produced by the drop impact and of the regions considered analytically.

gradients in the drop at the initial stage of the impact can be so high that the effect of viscosity cannot be neglected there. The effect of the viscosity becomes apparent in the viscous boundary layer near the wall. The velocity of the liquid outside the boundary layer is of order of the initial drop velocity U_0. The velocity field u near the wall can be estimated using the velocity distribution in the unsteady boundary layer corresponding to Stokes' first (or Rayleigh's) problem:

$$u = U_0 \,\mathrm{erf}\left(\frac{z}{2\sqrt{\nu t}}\right),$$

where erf(·) is the error function and z is the coordinate normal to the wall. The shear stress at the wall can be thus estimated as $\tau_w = U_0\rho\sqrt{\nu}/\sqrt{\pi t}$. The effect of the viscosity can be neglected when the inertial terms in the momentum of the liquid are much larger than the viscous drag forces ($\rho h_f U_0^2 \gg D_0\tau_w$). The last condition can be rewritten in the form

$$t \gg t_\nu = \frac{\nu D_0^2}{\pi h_f^2 U_0^2}.$$

It is convenient to write the above expression for the time t_ν in the non-dimensional form

$$\bar{t}_\nu = \frac{1}{\pi\,\bar{h}_f^2 Re}, \tag{1.2}$$

where the initial drop diameter D_0 is used as a length scale, and the parameter D_0/U_0 as a time scale; the variables with an overbar are dimensionless.

The proposed theory is valid when the time t_ν is smaller than the time of the initial drop deformation, which is of order of D_0/U_0, or in non-dimensional form if $\bar{t}_\nu < 1$.

In §2 the theory of Yarin & Weiss (1995) for the dynamics of the liquid film on the wall and the propagation of the kinematic discontinuity is generalized to the arbitrary non-axisymmetric case. Next, the equations of motion of the crown and rim are formulated. Also, an analytic expression for the shape of the crown is obtained for the case when the viscosity and surface tension are negligibly small. The theory is

applied to the cases of the normal impact of a single drop in § 3, and oblique impact of a single drop and the interaction of two crowns in § 4. The results are discussed in § 5, and conclusions are presented in § 6.

2. Formation and propagation of the upward jet: equations of motion for the arbitrary case

The solution of the problem of the jetting due to drop impact can be subdivided into five main parts. First, is the dynamics of motion of the liquid film on the wall. At the interface between different regions in the wall film the velocity gradients are very high. This interface is modelled in the present paper as a kinematic discontinuity. This kinematic discontinuity, where the velocity vector and the thickness of the film jump, is considered as a distributed volume sink Q. The second part of the solution is the consideration of the jump conditions for the velocity and the thickness of the film at the kinematic discontinuity and the derivation of the equations governing its propagation.

Next, when the local value of the volume sink Q is positive, a liquid film is ejected from the kinematic discontinuity. In this case the kinematic discontinuity is the base of the crown. The third part of the solution is the determination of the velocity and the thickness of this ejected film at the base of the crown. These values, as well as the location of the base of the crown are used as initial conditions to the equations of motion of the crown. Thus, the fourth part of the problem is the derivation of equations of motion of the upward jet.

The free upward jet is always bounded by a rim formed at its edge due to the surface tension. The description of the propagation of the rim is the fifth and conclusive part of the problem.

The general solution of the problem is given below. As was noted in § 1, the cases considered in the present work correspond to high Reynolds numbers and viscosity effects are neglected. The liquid is assumed to be incompressible.

2.1. *Dynamics of the liquid film on a plane rigid wall*

In the present section the quasi-one-dimensional theory of Yarin & Weiss (1995) is generalized to the case of a two-dimensional plane film. We consider the flow in a thin liquid film on a wall. The effects of the velocity component normal to the wall and of gravity are neglected. Following the simplified quasi-two-dimensional approach, the continuity equation of the film is

$$\frac{\partial h}{\partial t} + \nabla \cdot (h\boldsymbol{V}) = 0, \tag{2.1}$$

where h is the film thickness, t is the time, ∇ is the two-dimensional gradient operator in the plane parallel to the wall, and $\boldsymbol{V}$ is the average velocity vector over the film thickness and parallel to the wall.

The momentum equation of the film represents the balance between the inertial forces and surface tension. The effect of surface tension includes two forces. The first of these is the pressure distribution in the film. The inertial effects in the direction normal to the wall are negligibly small, and the average pressure over the film thickness is approximated by the local capillary pressure p_σ given as

$$p_\sigma = \sigma\kappa, \tag{2.2}$$

where σ is the surface tension and κ is the local curvature of the free surface of the film.

The second force is the surface tension force applied to the free surface of the film, $z = h$, and directed tangentially to this surface. However, the free surface (of zero mass) can be excluded from the momentum balance of the film and the second force can be substituted by the distribution of the capillary pressure $-p_\sigma \boldsymbol{n}$ over the surface $z = h$ ($\boldsymbol{n}$ being the local unit normal vector).

The projection of the surface tension forces on the plane of the wall yields the following momentum equation:

$$\rho \left[\frac{\partial h \boldsymbol{V}}{\partial t} + \nabla \cdot (h \boldsymbol{V} \otimes \boldsymbol{V}) \right] = -\nabla (h p_\sigma) + p_\sigma \nabla h, \tag{2.3}$$

where $\otimes$ denotes the tensor product. Note that equation (2.3), written for the planar or axisymmetric cases, is identical to the corresponding momentum equations given in Yarin & Weiss (1995).

Equation (2.3), using (2.1), can be reduced to the following form:

$$\rho \left[\frac{\partial \boldsymbol{V}}{\partial t} + (\boldsymbol{V} \cdot \nabla) \boldsymbol{V} \right] = -\nabla p_\sigma. \tag{2.4}$$

It can be shown that in cases when $|\nabla h| \ll 1$ equations (2.4) and (2.2) can be linearized and written in dimensionless form as

$$\left[\frac{\partial \overline{\boldsymbol{V}}}{\partial \bar{t}} + (\overline{\boldsymbol{V}} \cdot \overline{\nabla}) \overline{\boldsymbol{V}} \right] = \frac{1}{We} \overline{\nabla} (\overline{\nabla}^2 \bar{h}), \tag{2.5}$$

where the initial normal drop velocity, U_0, is used as a velocity scale, its initial diameter, D_0, is used as a length scale, and ∇^2 is the Laplace operator in two dimensions in the plane parallel to the wall.

The Weber number in the cases corresponding to the crown formation and splash is much larger than unity ($We \gg 1$). Therefore in a first-order approximation the capillary effects in the momentum equation, the right-hand side of (2.5), vanish and (2.4) takes the form

$$\frac{\mathrm{D} \boldsymbol{V}}{\mathrm{D} t} = 0, \tag{2.6}$$

where $\mathrm{D}/\mathrm{D}t$ denotes the material time derivative.

The solution of (2.6) in parametric form is therefore,

$$\boldsymbol{V} = \boldsymbol{F}(\boldsymbol{\zeta}), \quad \boldsymbol{x} = \boldsymbol{F}(\boldsymbol{\zeta})\, t + \boldsymbol{\zeta}, \tag{2.7a,b}$$

where $\boldsymbol{x}$ is the radius vector, and $\boldsymbol{F}$ is the initial value of the velocity vector $\boldsymbol{V}$ at the radius vector $\boldsymbol{\zeta}$.

The continuity equation (2.1) can be rewritten in the more convenient form

$$\frac{\mathrm{D} h}{\mathrm{D} t} = -h\, (\nabla \cdot \boldsymbol{V}). \tag{2.8}$$

The solution of (2.8), using (2.7), yields the following expression for the thickness of the film:

$$h(\boldsymbol{\zeta}) = \frac{h_0(\boldsymbol{\zeta})}{1 + (\nabla_\zeta \cdot \boldsymbol{F})\, t + \det(\nabla_\zeta \boldsymbol{F})\, t^2}, \tag{2.9}$$

where $\nabla_\zeta = \partial / \partial \boldsymbol{\zeta}$ denotes the gradient operator at the initial instant of time in the field with the radius vector defined by $\boldsymbol{\zeta}$, and $\nabla_\zeta \cdot \boldsymbol{F}$ is correspondingly the divergence

of the vector $\boldsymbol{F}$; h_0 is the initial distribution of the thickness. If in some $\boldsymbol{\zeta}$-region $\det(\nabla_\zeta \boldsymbol{F})$ is negative, the denominator on the right-hand side of (2.9) can vanish at some positive time instant t and, as noted in Yarin & Weiss (1995) and Whitham (1974), the solution produces a kinematic discontinuity. This kinematic discontinuity will be analysed in the next section.

It can also be shown that the expressions (1.1a, b) for the velocity and thickness of the film produced by a normal drop impact is a particular case of the solution (2.7) and (2.9) with

$$\bar{\boldsymbol{x}} = \bar{r}\,\boldsymbol{e}_r, \quad \bar{\boldsymbol{\zeta}} = \bar{\zeta}\,\boldsymbol{e}_r \quad \overline{\boldsymbol{F}} = \frac{\bar{\zeta}}{\bar{\tau}}\,\boldsymbol{e}_r \quad \bar{h}_0 = \frac{\bar{\eta}}{\bar{\tau}^2}.$$

2.2. *Propagation of the kinematic discontinuity on the wall*

Consider the liquid film on the wall surface, particularly regions 1 and 2 in figure 2. At the interface $\boldsymbol{X}_B$ between these two regions the thickness of the film jumps from h_1 to h_2 and the velocity from $\boldsymbol{V}_1$ to $\boldsymbol{V}_2$. This interface, which is the base of the upward jet (region 3 on figure 2) is treated in the theory of Yarin & Weiss (1995) as a kinematic discontinuity. The thickness and the height of this kinematic discontinuity is of order of the film thicknesses h_1 and h_2, and the rate of change of the mass of the discontinuity and the inertial effects associated with the acceleration of the kinematic discontinuity are neglected.

Denote by U the magnitude of the velocity of the discontinuity normal to its front. In the plane parallel to the wall consider a Cartesian coordinate system with the base unit vectors $\{\boldsymbol{e}_n, \boldsymbol{e}_\tau\}$ normal and tangent to the discontinuity front. The mass balance and the momentum equation of the kinematic discontinuity in the plane parallel to the wall can be written in the form

$$h_1(\boldsymbol{V}_1 - U\boldsymbol{e}_n)\cdot\boldsymbol{e}_n - h_2(\boldsymbol{V}_2 - U\boldsymbol{e}_n)\cdot\boldsymbol{e}_n = Q, \tag{2.10a}$$

$$h_1[(\boldsymbol{V}_1 - U\boldsymbol{e}_n)\cdot\boldsymbol{e}_n](\boldsymbol{V}_1 - U\boldsymbol{e}_n) - h_2[(\boldsymbol{V}_2 - U\boldsymbol{e}_n)\cdot\boldsymbol{e}_n](\boldsymbol{V}_2 - U\boldsymbol{e}_n) = Q(\boldsymbol{V}_d - U\boldsymbol{e}_n), \tag{2.10b}$$

where $\boldsymbol{V}_d$ is the velocity of the liquid at the discontinuity front and Q is the specific volume flux into the discontinuity (also called the sink strength at the discontinuity in Yarin & Weiss (1995)). If the viscous forces are negligibly small in comparison with the inertial forces, this velocity is equal to the centre-of-mass velocity

$$\boldsymbol{V}_d = \frac{\boldsymbol{V}_1 h_1 + \boldsymbol{V}_2 h_2}{h_1 + h_2}. \tag{2.11}$$

From (2.10) and (2.11) we arrive at

$$U = \tfrac{1}{2}(V_{n1} + V_{n2}), \quad Q = \tfrac{1}{2}(h_1 + h_2)\,(V_{n1} - V_{n2}). \tag{2.12a, b}$$

The shape of the discontinuity front can be defined in parametric form as

$$\boldsymbol{x} = \boldsymbol{X}_B(\xi, t), \tag{2.13}$$

where $\boldsymbol{x}$ is the radius vector, t is the time and ξ is a position parameter. It can be shown that the line defined as

$$\frac{\partial \boldsymbol{X}_B(\xi, t)}{\partial t} = \frac{\boldsymbol{V}_1(\boldsymbol{X}_B, t) + \boldsymbol{V}_2(\boldsymbol{X}_B, t)}{2} \tag{2.14}$$

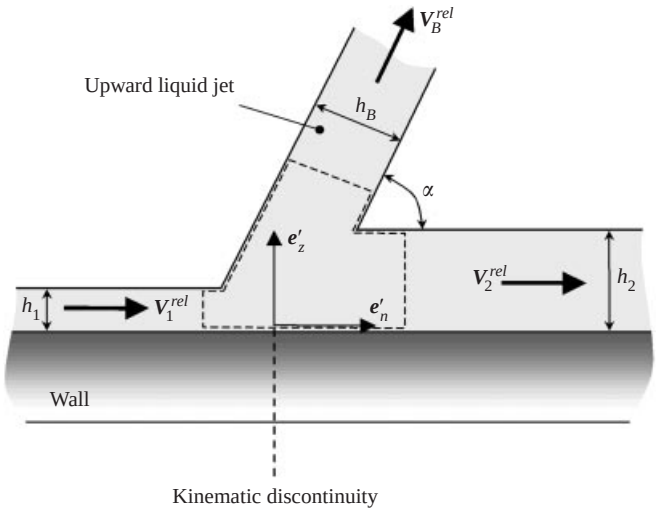

FIGURE 3. Sketch of the formation of the upward jet from the kinematic discontinuity.

moves normal to the discontinuity with the velocity U given in (2.12a). Equation (2.14) is the differential equation of the motion of the kinematic discontinuity, which can be integrated for given velocity fields $\boldsymbol{V}_1(\boldsymbol{x}, t)$ and $\boldsymbol{V}_2(\boldsymbol{x}, t)$.

2.3. *Liquid jet formed at the kinematic discontinuity*

If the strength of the sink Q determined in equation (2.12b) is positive, the interaction of two liquid flows on the wall results in an upward liquid jet at the kinematic discontinuity, as shown in figure 3.

A similar geometry of the splash was considered in Peregrine (1981). In that work a steady-state, one-dimensional model of the splash is developed. In the present model of the jetting, the general case is analysed, when the components of the film velocity parallel to the kinematic discontinuity do not vanish. Moreover, the surface tension effects are taken into account in the momentum equation.

Consider the Cartesian coordinate system $\{\boldsymbol{e}'_n, \boldsymbol{e}'_\tau, \boldsymbol{e}'_z\}$ moving the discontinuity front with velocity

$$\boldsymbol{V}_{cs} = U\boldsymbol{e}'_n + \frac{V_{\tau 1} + V_{\tau 2}}{2}\,\boldsymbol{e}'_\tau. \tag{2.15}$$

Here the base unit vectors $\boldsymbol{e}'_n$ and $\boldsymbol{e}'_\tau$ are normal and tangent to the kinematic discontinuity, and the base unit vector $\boldsymbol{e}'_z$ is normal to the wall. The velocity U, defined in (2.12a), is the velocity of propagation of the discontinuity in the normal, $\boldsymbol{e}'_n$, direction, and $V_{\tau 1}$ and $V_{\tau 2}$ are the tangential components of the velocity of the liquid in the films with thicknesses h_1 and h_2, respectively.

The velocities of the liquid on the wall from the two sides of the discontinuity in this coordinate system are

$$\boldsymbol{V}_1^{rel} = \frac{V_{n1} - V_{n2}}{2}\,\boldsymbol{e}'_n + \frac{V_{\tau 1} - V_{\tau 2}}{2}\,\boldsymbol{e}'_\tau = -\boldsymbol{V}_2^{rel}. \tag{2.16}$$

Denote by α the angle of inclination of the jet to the wall in the coordinate system $\{\boldsymbol{e}'_n, \boldsymbol{e}'_\tau, \boldsymbol{e}'_z\}$. Thus, the unit vector $\boldsymbol{e}_J$ in the direction of the upward jet can be defined as

$$\boldsymbol{e}_J = \boldsymbol{e}'_n \cos\alpha + \boldsymbol{e}'_z \sin\alpha. \tag{2.17}$$

Assuming the pressure to be constant, neglecting the rate of the mass change accumulated inside the kinematic discontinuity and the inertial effects of this mass, the mass balance, the axial momentum balance in the normal and tangential directions, and the Bernoulli equation at the base of the crown can be written in the following form:

$$-h_1 \boldsymbol{V}_1^{rel} \cdot \boldsymbol{e}_n' + h_B \boldsymbol{V}_B^{rel} \cdot \boldsymbol{e}_J + h_2 \boldsymbol{V}_2^{rel} \cdot \boldsymbol{e}_n' = 0, \tag{2.18a}$$

$$\left[-\rho h_1 (\boldsymbol{V}_1^{rel} \cdot \boldsymbol{e}_n') \boldsymbol{V}_1^{rel} + \rho h_B (\boldsymbol{V}_B^{rel} \cdot \boldsymbol{e}_J) \boldsymbol{V}_B^{rel} + \rho\, h_2 (\boldsymbol{V}_2^{rel} \cdot \boldsymbol{e}_n') \boldsymbol{V}_2^{rel}\right] \cdot \boldsymbol{e}_n' = 2\sigma \cos\alpha, \tag{2.18b}$$

$$\left[-\rho h_1 (\boldsymbol{V}_1^{rel} \cdot \boldsymbol{e}_n') \boldsymbol{V}_1^{rel} + \rho h_B (\boldsymbol{V}_B^{rel} \cdot \boldsymbol{e}_J) \boldsymbol{V}_B^{rel} + \rho h_2 (\boldsymbol{V}_2^{rel} \cdot \boldsymbol{e}_n') \boldsymbol{V}_2^{rel}\right] \cdot \boldsymbol{e}_\tau' = 0, \tag{2.18c}$$

$$\boldsymbol{V}_1^{rel} \cdot \boldsymbol{V}_1^{rel} = \boldsymbol{V}_B^{rel} \cdot \boldsymbol{V}_B^{rel}, \tag{2.18d}$$

$$\boldsymbol{V}_1^{rel} \cdot \boldsymbol{V}_1^{rel} = \boldsymbol{V}_2^{rel} \cdot \boldsymbol{V}_2^{rel}, \tag{2.18e}$$

where h_B is the thickness of the crown at its base, α is the inclination angle at the base, and $\boldsymbol{V}_B^{rel}$ is the velocity of the liquid in the inclined jet at the base relative to the coordinate system $\{\boldsymbol{e}_n', \boldsymbol{e}_\tau', \boldsymbol{e}_z'\}$. The mass balance (2.18*a*) expresses the fact that the sum of the volume fluxes of the fluid entering into the kinematic discontinuity must vanish. The momentum equations (2.18*b*, *c*) express the balance of the inertial and surface tension forces in the plane parallel to the wall. The Bernoulli equations (2.18*d*, *e*) use the the fact that the pressure p_0 in the films of thickness h_1 and h_2, as well as in the crown outside the kinematic discontinuity, is equal to the constant pressure in the surrounding air. Note that the choice of the coordinate system $\{\boldsymbol{e}_n', \boldsymbol{e}_\tau', \boldsymbol{e}_z'\}$ moving with the velocity (2.15) was partially to satisfy condition (2.18*e*) automatically.

Note, also, that the upward jet appears at the kinematic discontinuity because the pressure inside this discontinuity differs from p_0. Moreover, the vertical reaction of the wall per unit length of the discontinuity, F_p, associated with this pressure, can be estimated using the momentum balance equation in the z-direction:

$$F_p = \rho h_B (\boldsymbol{V}_B^{rel} \cdot \boldsymbol{e}_J)(\boldsymbol{V}_B^{rel} \cdot \boldsymbol{e}_z) - 2\sigma \sin\alpha.$$

Equations (2.18) are similar to the relations between the streams appearing due to the splash derived in Peregrine (1981). However, the non-stationary inertial effects are neglected in the analysis of Peregrine (1981) and, as a result, the theory predicts the steady motion of the base of the crown. This result is not confirmed by the experimental observations which can be expressed well by (1.1).

In the present analysis only the terms associated with the acceleration of the kinematic discontinuity are neglected. The width and the height of this region are of order of magnitude h, which is the characteristic thickness of the liquid on the wall. The condition that the non-stationary terms inside the kinematic discontinuity can be neglected is therefore

$$\rho h\, (V^{rel})^2 \gg \rho h^2\, \frac{\mathrm{d}V_{cs}}{\mathrm{d}t}. \tag{2.19}$$

The condition (2.19) applied to the case of the normal impact of a single drop onto a stationary liquid film of the thickness h_f yields, with the help of (1.1), the condition $\bar{h}_f / \overline{R}_B \ll 1$. Therefore, the inertial effects of the liquid inside the kinematic discontinuity can indeed be neglected in the remote asymptotic solution considered in the present work.

The velocity vector $\boldsymbol{V}_B^{rel}$ must be parallel to the jet. This means that this velocity

can be written in the form

$$\boldsymbol{V}_B^{rel} = V_{JB}^{rel}\,\boldsymbol{e}_J + V_{\tau B}^{rel}\,\boldsymbol{e}'_\tau,$$

where the unit vector $\boldsymbol{e}_J$ is defined in (2.17). The solution of the system of equations (2.18*a–d*) with the help of (2.16) yields the following expressions for the velocity of the liquid in the jet at the base of the crown, its thickness and the inclination angle in the moving coordinate system $\{\boldsymbol{e}'_n, \boldsymbol{e}'_\tau, \boldsymbol{e}'_z\}$:

$$V_{\tau B}^{rel} = \frac{h_1 - h_2}{h_1 + h_2} V_{\tau 1}^{rel}, \tag{2.20a}$$

$$V_{JB}^{rel} = \left[(V_{n1}^{rel})^2 + \frac{4h_1h_2}{(h_1+h_2)^2}(V_{\tau 1}^{rel})^2\right]^{1/2}, \tag{2.20b}$$

$$h_B = \frac{(h_1+h_2)V_{n1}^{rel}}{V_{JB}^{rel}}, \tag{2.20c}$$

$$\cos\alpha = \frac{(h_1-h_2)(V_{n1}^{rel})^2}{(h_1+h_2)\,V_{n1}^{rel}\,V_{JB}^{rel} - 2\sigma/\rho}. \tag{2.20d}$$

The final expressions for the velocity of the jet at the base in the laboratory coordinate system $\{\boldsymbol{e}_n, \boldsymbol{e}_\tau, \boldsymbol{e}_z\}$ and its thickness are obtained using (2.12), (2.15) and (2.20*a*):

$$\boldsymbol{V}_B = \frac{\boldsymbol{V}_1h_1 + \boldsymbol{V}_2h_2}{h_1+h_2} + \frac{2\sigma}{\rho Q}\cos\alpha\,\boldsymbol{e}_n + \frac{S}{2(h_1+h_2)}\sin\alpha\,\boldsymbol{e}_z, \tag{2.21a}$$

$$h_B = \frac{(h_1+h_2)^2\,(V_{n1}-V_{n2})}{S}, \tag{2.21b}$$

where the function S and the angle α are defined as

$$S = \sqrt{(h_1+h_2)^2(V_{n1}-V_{n2})^2 + 4h_1h_2(V_{\tau 1}-V_{\tau 2})^2}, \tag{2.22a}$$

$$\alpha = \arccos\left[\frac{(h_1-h_2)\,(V_{n1}-V_{n2})^2}{(V_{n1}-V_{n2})\,S - 8\sigma/\rho}\right], \tag{2.22b}$$

and Q is determined in (2.12).

The absolute value of the argument of the cosine function in the right-hand side of equation (2.22*b*) should be smaller than unity. Otherwise, a solution for α does not exist and the crown is not formed. It can be shown that a solution for the angle α always exists in the asymptotic case $\sigma = 0$. Consider for simplicity case $\sigma > 0$ for the example of axisymmetric geometry of the impact ($V_{\tau 1} = V_{\tau 2} = 0$). Equations (2.21*b*) and (2.22*b*) can be reduced to the form

$$h_B = h_1 + h_2, \quad \alpha = \arccos\left[\frac{(h_1-h_2)(V_{n1}-V_{n2})^2}{h_B(V_{n1}-V_{n2})^2 - 8\sigma/\rho}\right],$$

and the necessary condition for formation of the crown is $8\sigma/\rho < \min(h_1, h_2)$ $(V_{n1}-V_{n2})^2$. This condition is not satisfied after an impact with a low Weber number. In this case, the inertial forces are weak in comparison with the surface tension forces, preventing creation of the crown. In the present paper only impacts with high Weber numbers are considered, when the inertia plays a dominant role in the force balance.

Expressions (2.21) together with the position of the crown base $\boldsymbol{X}_B$ obtained by integration of (2.14) can be used as initial conditions for the determination of the shape of the jet. The dynamic equations of propagation of the jet are given below.

2.4. *Surface of the crown and its thickness*

The surface of the jet is assumed to be thin. The radius vector corresponding to the median surface of the jet (see figure 2) can be defined in the Lagrangian form for any instant in time t as $\boldsymbol{X}_J(\xi, t_B, t)$, where ξ is a position parameter, t_B is the time instant at which the material point located at $\boldsymbol{X}_J$ is ejected from the wall (at the base of the crown) such that

$$\boldsymbol{X}_J(\xi, t_B, t_B) = \boldsymbol{X}_B(\xi, t_B). \tag{2.23}$$

Parameter ξ is associated with the position of the given material point along the front of the kinematic discontinuity $\boldsymbol{X}_B$.

The equation of motion of the material point of the jet is in its general form

$$\rho\, h_J\, \partial A_J\, \frac{\partial^2}{\partial t^2} \boldsymbol{X}_J(\xi, t_B, t) = \partial \boldsymbol{T}, \tag{2.24}$$

where h_J is the local thickness of the jet, ∂A_J is the element of the jet surface, $\partial \boldsymbol{T}$ is the total force applied to that element of the jet, including in general the capillary, viscous, body forces and the gas drag force. The details of the force $\partial \boldsymbol{T}$ applied to the element of a free-moving sheet, as well as the quasi-two-dimensional equations of the motion of the free liquid film can be found in Yarin (1993).

The effect of the surface tension consists of the capillary pressure in the film and the δ-functional surface tension force acting at the two free surfaces bounding the considered element of the area ∂A_J. The effect of the capillary pressure can be neglected in a free thin film. The δ-functional surface tension force at each free side of the jet can be substituted by a resulting force $\sigma\kappa\partial A_J \boldsymbol{n}_J$, where κ is the local curvature of the jet and $\boldsymbol{n}_J$ is the unit normal vector directed towards the centre of curvature.

In the present analysis the effect of viscosity is neglected and the momentum balance equation of the upward jet takes the form

$$\frac{\partial^2}{\partial t^2} \boldsymbol{X}_J(\xi, t_B, t) = \frac{2\sigma\kappa}{\rho h_J}\, \boldsymbol{n}_J - g\boldsymbol{e}_z, \tag{2.25}$$

where g is the acceleration due to gravity.

Consider now the thickness $h_J(\xi, t_B, t)$ of the jet. Conservation of mass of the element of the crown yields

$$h_B(\xi, t_B)\, \partial A_J(\xi, t_B, t_B) = h_J(\xi, t_B, t)\, \partial A_J(\xi, t_B, t), \tag{2.26}$$

where the element of the area of the jet, ∂A_J, can be defined as

$$\partial A_J = \left| \frac{\partial \boldsymbol{X}_J}{\partial \xi} \times \frac{\partial \boldsymbol{X}_J}{\partial t_B} \right| \partial\xi\, \partial t_B. \tag{2.27}$$

Equations (2.26) and (2.27) yield the following expression for the thickness of the jet:

$$h_J(\xi, t_B, t) = h_B(\xi, t_B)\, \frac{|(\partial/\partial\xi)\boldsymbol{X}_J(\xi, t_B, t) \times (\partial/\partial t_B)\boldsymbol{X}_J(\xi, t_B, t)|_{|t=t_B}}{|(\partial/\partial\xi)\boldsymbol{X}_J(\xi, t_B, t) \times (\partial/\partial t_B)\boldsymbol{X}_J(\xi, t_B, t)|}. \tag{2.28}$$

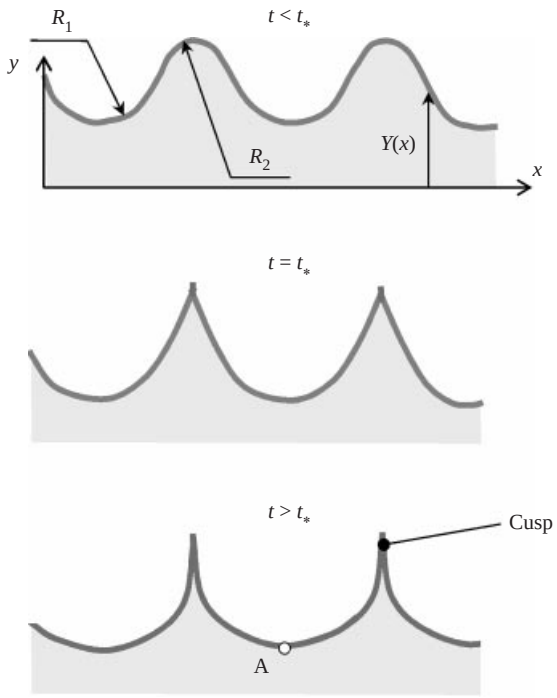

FIGURE 4. Sketch of the rim instability and cusp formation.

In order to calculate the shape of the jet and its thickness, equation (2.25) must be integrated with the help of (2.28) subject to the initial conditions at the base of the crown:

$$t = t_B: \qquad \boldsymbol{X}_J = \boldsymbol{X}_B(\xi, t_B), \quad \frac{\partial \boldsymbol{X}_J}{\partial t} = \boldsymbol{V}_B(\xi, t_B), \quad h_J = h_B(\xi, t_B). \tag{2.29}$$

2.5. *Free rim bounding the jet*

The jet is bounded by the free rim (see figure 2) whose location is denoted here as X_R. The formation of a rim at the edge of a liquid film is a typical phenomenon first described theoretically by Taylor (1959) for a free liquid film of uniform thickness and constant velocity. The mass balance and momentum balance equations of the stationary rim for an arbitrary velocity field in the film can be also found in Yarin (1993). However, if the mass of the rim is small, the inertial effects associated with the acceleration of the rim and the flow inside the rim can be neglected. Also, if the radius of the curvature of the centreline of the rim is much larger than the characteristic size of its cross-section, the velocity of the rim relative to the liquid in the film can be approximated well by the expression obtained by Taylor (1959):

$$U_R = \sqrt{\frac{2\sigma}{\rho\, h_R}}, \tag{2.30}$$

where h_R is the film thickness near the rim.

In the study of Yarin & Weiss (1995) the loss of the rim stability and formation of jets is explained by a cusp formation. Consider small perturbations $Y(x,t)$ of the rim centreline (figure 4). The velocity of the rim propagation relative to a free liquid film

is given by (2.30). The height of the rim can be thus described by

$$\frac{\partial Y}{\partial t} = -U_R\sqrt{1+\left(\frac{\partial Y}{\partial x}\right)^2}. \tag{2.31}$$

Equation (2.31) is the eikonal equation which has an analytical solution obtained in Whitham (1974, pp. 241–243) using the integration of the equation along the characteristic curves. Moreover, it was shown that these curves, characteristic for the equation (2.31), are actually straight lines normal to the initial shape of the rim centreline. Denote $\boldsymbol{X}_0 = x\,\boldsymbol{e}_x + Y_0(x)\,\boldsymbol{e}_y$ as the initial shape of the rim. Its position at the time instant t can be expressed in the parametric form $\boldsymbol{X}(x_0,t) = x(x_0,t)\,\boldsymbol{e}_x + Y(x_0,t)\,\boldsymbol{e}_y$ with

$$x(x_0,t) = x_0\left[\frac{Y_0'(x_0)U_r t}{\sqrt{1+Y_0'^2(x_0)}}+1\right], \tag{2.32a}$$

$$Y(x_0,t) = Y_0(x_0) - \frac{U_r t}{\sqrt{1+Y_0'^2(x_0)}}, \tag{2.32b}$$

where the parameter x_0 represents the initial position of the point considered along the characteristic line, and the prime in $Y_0'(x_0)$ denotes the derivative with respect to x_0.

Consider now the radius of curvature $R(x_0)$ of the rim centreline $\boldsymbol{X}(x_0,t)$:

$$R(x_0,t) = -\frac{[x'^2(x_0,t)+Y'^2(x_0,t)]^{3/2}}{x'(x_0,t)Y''(x_0,t)-x''(x_0,t)Y'(x_0,t)}. \tag{2.33}$$

The prime in (2.33) denotes the partial derivative with respect to x_0. The sign in (2.33) is chosen such that the radius R at the points where the rim is concave outward is positive (equal to the radius R_2 defined in figure 4).

Substituting the expressions (2.32) for the coordinates of the rim into (2.33) yields the following expression for the radius of curvature:

$$R(x_0,t) = R_0(x_0) - U_r t, \tag{2.34}$$

where $R_0(x_0) = R(x_0,0)$ is the initial curvature radius of the rim centreline.

Therefore, if the initial radius of curvature is negative (radius R_1 in figure 4), its absolute value increases with time. If the initial radius of curvature is positive (radius R_2 in figure 4), its absolute value decreases and vanishes at some time instant t_*. The instant t_* when the radius of curvature R_2 vanishes corresponds to the cusp formation and the beginning of the jetting and splash. The time instant t_* can be estimated as

$$t_* = R_0\sqrt{\rho h_J/\sigma}.$$

At times larger than t_* the liquid flows from the rim to jets, which then break up into secondary droplets. The radius of the cross-section of the rim does not grow significantly and the inertial effects associated with the mass of the rim per unit length can be neglected. This means that even after the time instant t_* the velocity of the rim at point A in figure 4 can be approximated by equation (2.30).

2.6. *Approximation for high We*

Note that, if the impact velocity is so high that surface tension effects are negligibly small in comparison to the inertial effects, in other words, if the Weber number is

sufficiently larger than unity, the expression (2.21a) for the velocity $\boldsymbol{V}_B$ of the ejected liquid at the kinematic discontinuity can be reduced to the following form:

$$\boldsymbol{V}_B = \frac{\boldsymbol{V}_1 h_1 + \boldsymbol{V}_2 h_2}{h_1 + h_2} + |\boldsymbol{V}_1 - \boldsymbol{V}_2| \, \frac{\sqrt{h_1 \, h_2}}{h_1 + h_2} \, \boldsymbol{e}_z. \tag{2.35}$$

The equation of motion of the jet can be reduced to the form

$$\frac{\partial^2}{\partial t^2} \boldsymbol{X}_J(\xi, t_B, t) = -g \, \boldsymbol{e}_z, \tag{2.36}$$

the solution of which is

$$\boldsymbol{X}_J(\xi, t_B, t) = \boldsymbol{X}_B(\xi, t_B) + \boldsymbol{V}_B(\xi, t_B) \, (t - t_B) - \frac{g(t - t_B)^2}{2} \, \boldsymbol{e}_z. \tag{2.37}$$

3. Normal impact of a single drop on a wetted surface

Consider a liquid drop of diameter D_0 impacting with the impact velocity U_0 on a stationary liquid film of constant thickness h_f. If the impact velocity is high enough, the initial deformation of the drop and of the film is followed by the formation of a crown-like jet. The geometry considered is axisymmetric, therefore the base of the crown is an expanding circle with the centre at the point of impact. The components of the velocities in the film normal to the kinematic discontinuity are equal to the radial velocities, and the tangential components vanish.

Consider the cylindrical coordinate system $\{r, \phi, z\}$ with base vectors $\{\boldsymbol{e}_r, \boldsymbol{e}_\phi, \boldsymbol{e}_z\}$ and the origin fixed at the point of impact. Assume that the impact velocity is so high that the viscous and surface tension effects are negligibly small in comparison to the inertia of the liquid. The theory of Yarin & Weiss (1995) describes the velocity inside the kinematic discontinuity and the thickness of the film at times sufficiently larger than D_0/U_0 in the dimensionless form (1.1a, b), whereas the film of the thickness h_f outside the kinematic discontinuity remains undisturbed. It can be shown that the solution of (2.14) in this case yields the radius of the kinematic discontinuity in the form of (1.1c). The velocity and thickness of the jet at the kinematic discontinuity can be obtained in dimensionless form by substituting (1.1) into (2.35) and (2.21ab) and neglecting the terms associated with the surface tension:

$$\boldsymbol{V}_B(t) = \frac{\beta \, \eta^{1/2}}{(t + \tau)^{1/2} \, [\eta + h_f \, (t + \tau)^2]} \, (\eta^{1/2} \, \boldsymbol{e}_r + h_f^{1/2} \, (t + \tau) \, \boldsymbol{e}_z), \tag{3.1a}$$

$$h_B(t) = \frac{\eta}{(t + \tau)^2} + h_f. \tag{3.1b}$$

Here the drop diameter D_0 is used as a length scale, the impact velocity U_0 as a velocity scale, and D_0/U_0 as a time scale. From here on the overbar denoting a dimensionless variable is dropped.

In the right-hand side of the equation of motion of the crown (2.21) only gravity effects are taken into account. In this case an analytic solution for the shape of the crown is derived in the form

$$\boldsymbol{X}_J(t_B, t) = \beta(t_B + \tau)^{1/2} \left[1 + \frac{\eta}{(t_B + \tau) \, [\eta + h_f \, (t_B + \tau)^2]} \, (t - t_B)\right] \boldsymbol{e}_r$$
$$+ \beta(t_B + \tau)^{1/2} \, \frac{\eta^{1/2} \, h_f^{1/2}}{\eta + h_f (t_B + \tau)^2} \, (t - t_B) \boldsymbol{e}_z - \frac{Fr^{-1}}{2} \, (t - t_B)^2 \, \boldsymbol{e}_z, \tag{3.2}$$

where the Froude number is defined as

$$Fr = \frac{U_0^2}{g\, D_0}.$$

The solution for the thickness of the crown is obtained by substituting (3.2) in (2.28), taking the azimuthal angle ϕ as parameter ξ and accounting for the axial symmetry of the problem:

$$h_J(t_B, t) = h_B(t_B)\, \frac{R_B(t_B)}{R_J(t_B, t)}\, \frac{\sqrt{G_1^2\,(t_B, t_B) + G_2^2\,(t_B, t_B)}}{\sqrt{G_1^2\,(t_B, t) + G_2^2\,(t_B, t)}}, \tag{3.3}$$

where the radius of the crown and the functions G_1 and G_2 are defined as

$$R_J(t_B, t) = \beta\,(t_B + \tau)^{1/2} \left[1 + \frac{\eta}{(t_B + \tau)[\eta + h_f(t_B + \tau)^2]}(t - t_B)\right], \tag{3.4a}$$

$$G_1(t_B, t) = \frac{1}{2(\tau + t_B)^{3/2}} \left[\tau + t_B + \frac{4(t - t_B)\eta^2}{[\eta + h_f(t_B + \tau)^2]^2} + \frac{\eta(3t_B - 5t - 2\tau)}{\eta + h_f(t_B + \tau)^2}\right] \tag{3.4b}$$

and

$$G_2(t_B, t) = \frac{(t - t_B)}{AFr} + \frac{(\eta h_f)^{1/2}[h_f t_B^3 - (3t_B + 2\tau)(\eta + h_f\tau^2) + t(\eta - 3h_f(t_B + \tau)^2)]}{2(\tau + t_B)^{1/2}\,[\eta + h_f(\tau + t_B)^2]^2}. \tag{3.4c}$$

Consider now the rim bounding the crown and defining its height. We assume the centreline of the rim to be a circle defined as $\boldsymbol{x} = \boldsymbol{X}_R(t)$. The rim belongs to the crown, therefore the rim location can be expressed in the form

$$\boldsymbol{X}_R(t) = \boldsymbol{X}_J(t_R, t), \tag{3.5}$$

where parameter t_R is a function of time t. Expression (3.5) also means that a material point located at the time instant t_R at the kinematic discontinuity reaches the rim at the instant t. Denote W_R as the total volume of liquid ejected from the film to the jet at the kinematic discontinuity in the time interval from zero to t_R:

$$W_R(t_R) = 2\pi \int_0^{t_R} R_B(t) Q(t)\, \mathrm{d}t. \tag{3.6}$$

Using the mass balance, at time instant t this entire volume $W_R(t_R)$ is accumulated in the rim or ejected from the rim to the jets and to the secondary droplets. If we assume that the rim moves with the velocity (2.30) relative to the liquid in the crown, the total volume flux can be obtained as

$$\frac{\mathrm{d}W_R}{\mathrm{d}t} = 2\pi R_R(t) h_R(t) U_R(t), \tag{3.7}$$

where R_R is the dimensionless radius of the centreline of the rim.

On the other hand, differentiating (3.6) with respect to t_R yields

$$\frac{\mathrm{d}W_R}{\mathrm{d}t_R} = 2\pi R_B(t_R) Q(t_R). \tag{3.8}$$

Equations (3.7) and (3.8) lead to the following differential equation for the time t_R:

$$\frac{\mathrm{d}t_R(t)}{\mathrm{d}t} = \frac{R_R(t) h_R(t) U_R(t)}{R_B(t_R) Q(t_R)}. \tag{3.9}$$

Equation (3.5), using (1.1), (2.14) and (2.30), yields

$$\frac{\mathrm{d}t_R(t)}{\mathrm{d}t} = \sqrt{\frac{8}{We}}\,\frac{R_R(t)h_R^{1/2}(t)}{\beta^2 h_B(t_R)}, \tag{3.10}$$

where the radius of the centreline of the rim and the thickness of the jet at the rim are defined as

$$R_R(t) = \boldsymbol{X}_J(t_R, t)\cdot\boldsymbol{e}_r,$$
$$h_R(t) = h_J(t_R, t),$$

respectively.

4. Non-axisymmetric cases

4.1. *Oblique impact of a single drop*

In this section the theory described in § 2 is applied to the case of impact of a single drop on a uniform film moving with the constant velocity $\boldsymbol{V}_\tau$. The impact velocity $\boldsymbol{U}_0$ is directed normal to the wall. The initial diameter of the drop is denoted D_0. The impact angle θ is defined here as $\tan\theta = V_\tau/U_0 = \overline{V}_\tau$. The axisymmetric case considered in § 3 corresponds to an angle of zero.

Consider the Cartesian coordinate system $\{x, y, z\}$ with the base vectors $\{\boldsymbol{e}_x, \boldsymbol{e}_y, \boldsymbol{e}_z\}$ fixed at the point of impact, axis x is directed opposite to $\boldsymbol{V}_\tau$, axis z is normal to the wall. The velocity $\boldsymbol{V}_l$ in the lamella inside the crown (1.1*a*), which is assumed to be uninfluenced by the outer flow, and the velocity $\boldsymbol{V}_f$ in the outer undisturbed film are written in this coordinate system in dimensionless form as

$$\boldsymbol{V}_l = \frac{1}{t+\tau}\,(x\boldsymbol{e}_x + y\boldsymbol{e}_y), \tag{4.1a}$$

$$\boldsymbol{V}_f = -V_\tau\,\boldsymbol{e}_x, \tag{4.1b}$$

where, as in § 3, D_0 is used as a length scale and U_0 is used as a velocity scale. Here and below the overbar denoting a dimensionless variable is dropped.

The thickness h_l of the inner film is expressed in the form (1.1*b*), whereas the thickness h_f of the outer film is constant.

The solution of the equation of propagation of the base of the crown (2.14) can be obtained with the help of (4.1) and (1.1*b*) in the form

$$\boldsymbol{X}_B = [-V_\tau(t+\tau) + C_1\sqrt{t+\tau}]\,\boldsymbol{e}_x + C_2\sqrt{t+\tau}\,\boldsymbol{e}_y, \tag{4.2}$$

where C_1 and C_2 are integration constants which must be found from the initial conditions.

Assuming an elliptical initial shape of the kinematic discontinuity just after the initial deformation of the drop, at the time of order $t \approx 1$, the solution (4.2) yields the shape of the kinematic discontinuity in the following parametric form:

$$\boldsymbol{X}_B(\varphi, t) = \left[\beta_x\cos\varphi\sqrt{t+\tau} - V_\tau(t+\tau) + V_\tau\sqrt{1+\tau}\sqrt{t+\tau} + x_0\frac{\sqrt{t+\tau}}{\sqrt{1+\tau}}\right]\boldsymbol{e}_x$$
$$+\beta_y\sin\varphi\sqrt{t+\tau}\,\boldsymbol{e}_y, \tag{4.3}$$

where $\varphi \in [-\pi,\ \pi]$ is the circumferential parameter, x_0 is the displacement of the centre of the initial ellipse at the instant $t \approx 1$; $\beta_x > 0$, $\beta_y > 0$ and τ are non-dimensional constants. It is interesting that the shape of the kinematic discontinuity (4.3) remains elliptic. The half-axes of the ellipse are $\beta_x\sqrt{1+\tau}$ and $\beta_y\sqrt{1+\tau}$, and the ratio between these two half-axes is constant: $\gamma = \beta_y/\beta_x$.

The unit vector $\boldsymbol{n}$ normal to the ellipse $\boldsymbol{X}_B$ is now expressed in the form

$$\boldsymbol{n} = \frac{\gamma\ \cos\varphi\ \boldsymbol{e}_x + \sin\varphi\ \boldsymbol{e}_y}{\sqrt{\gamma^2\ \cos^2\varphi + \sin^2\varphi}}. \tag{4.4}$$

Therefore the strength of the sink Q can be obtained in dimensionless form using (2.12), (4.1), (4.3) and (4.4) as

$$Q = \frac{(h_1 + h_2)\ (\beta_x + B\cos\varphi)\ \gamma}{2\sqrt{t+\tau}\ \sqrt{\gamma^2\ \cos^2\varphi + \sin^2\varphi}}, \tag{4.5a}$$

where

$$B = V_\tau\sqrt{1+\tau} + \frac{x_0}{\sqrt{1+\tau}}. \tag{4.5b}$$

Note that the flux Q, defined in (4.5), is positive everywhere on the kinematic discontinuity only if $\beta_x > B$. In this case the base of the crown is a closed ellipse expressed by (4.3). Otherwise, the jet is formed only on the part of the ellipse corresponding to $\varphi \in [-\varphi^*, \varphi^*]$ where

$$\varphi^* = \arccos(-\beta_x/B). \tag{4.6}$$

The velocity of the jet at the kinematic discontinuity is approximated using (2.35) by

$$\boldsymbol{V}_B(\varphi, t) = \frac{h_l\ \boldsymbol{X}_B(\varphi, t)}{(h_l + h_f)(t+\tau)} - \frac{h_f V_\tau}{h_l + h_f}\ \boldsymbol{e}_x + \frac{\sqrt{h_l h_f}\sqrt{(\beta\cos\varphi + B)^2 + \gamma^2\beta^2\sin^2\varphi}}{(h_l + h_f)\sqrt{t+\tau}}\ \boldsymbol{e}_z. \tag{4.7}$$

The crown in the case of oblique impact is a three-dimensional expanding surface. It can be given in parametric form using (4.3), (4.7), and the parameter φ instead of ξ in (2.37).

In the present analysis we do not consider the motion of the rim, which in the case of oblique impact is a complex three-dimensional curve. Nevertheless, the shape of the crown obtained can be used as an asymptotic shape for the case $We \to \infty$.

4.2. *Interaction of two crowns*

Consider two drops of diameter D_1 and $D_2 = k_d\ D_1$ impacting normally onto a wetted wall with the impact velocities U_1 and $U_2 = k_u\ U_1$. The constant thickness of the film before impact is h_f and its velocity is $\boldsymbol{V}_f = 0$.

Consider also a Cartesian coordinate system $\{x, y\}$ in the plane of the wall with the base vectors $\{\boldsymbol{e}_x, \boldsymbol{e}_y\}$. The first drop impacts at the origin of the coordinate system $(0, 0)$, the second at point $(\Delta x, 0)$. Denote Δt as the time interval between impacts. Each impacting drop disturbs the film on the wall and produces a spot with radially expanding flow. This flow is analysed in the theory of Yarin & Weiss (1995) and is defined in (1.1). In our coordinate system the velocities $\boldsymbol{V}_1$ and $\boldsymbol{V}_2$, the thicknesses h_1 and h_2 of the film in these spots, as well as the crown radii R_{B1} and R_{B2} can be written in the dimensionless form

$$\boldsymbol{V}_1 = \frac{x\ \boldsymbol{e}_x + y\ \boldsymbol{e}_y}{t+\tau_1}, \quad \boldsymbol{V}_2 = \frac{(x-\Delta x)\ \boldsymbol{e}_x + y\ \boldsymbol{e}_y}{t+\tau_2}, \tag{4.8a,b}$$

$$h_1 = \frac{\eta_1}{(t+\tau_1)^2}, \quad h_2 = \frac{\eta_2}{(t+\tau_2)^2}, \tag{4.8c,d}$$

$$R_{B1} = \beta_1\ (t+\tau_1)^{1/2}, \quad R_{B2} = \beta_2\ (t+\tau_2)^{1/2}, \tag{4.8e,f}$$

where D_1 is used as a scale for the length and U_1 as a scale for the velocity. Note that the non-dimensional parameters β_1, τ_1 and η_1 are in general functions of the Reynolds number, $Re_1 = \rho\ U_1\ D_1/\mu$, Weber number, $We_1 = \rho\ U_1^2\ D_1/\sigma$, and the dimensionless film thickness h_f:

$$\beta_1 = \beta(Re_1, We_1, h_f), \quad \tau_1 = \tau(Re_1, We_1, h_f), \quad \eta_1 = \eta(Re_1, We_1, h_f),$$

whereas the parameters β_2, τ_2 and η_2 are defined as

$$\beta_2 = \sqrt{k_u\ k_d}\ \beta(Re_2, We_2, h_f/k_d), \quad \tau_2 = \frac{k_u}{k_d}\ \tau(Re_2, We_2, h_f/k_d) - \Delta t, \tag{4.9a,b}$$

$$\eta_2 = \frac{k_d^3}{k_u}\ \eta(Re_2, We_2, h_f/k_d), \tag{4.9c}$$

with $Re_2 = \rho\ U_2\ D_2/\mu$ and $We_2 = \rho\ U_2^2\ D_2/\sigma$. Functions β, τ and η correspond to single drop impact.

The initial instant t_0 of intersection of the bases of the two crowns can be found from the condition

$$R_{B1} + R_{B2} = \Delta x,$$

which with the help of (4.8*e*,*f*) yields

$$t_0 = \frac{(\beta_1^2 + \beta_2^2)\Delta x^2 - \beta_1^4\tau_1 - \beta_2^4\tau_2 + \beta_1^2\beta_2^2(\tau_1 + \tau_2)}{(\beta_1^2 - \beta_2^2)^2} - \frac{2\beta_1\beta_2\Delta x\sqrt{\Delta x^2 - (\beta_1^2 - \beta_2^2)(\tau_1 - \tau_2)}}{(\beta_1^2 - \beta_2^2)^2}$$

if $\beta_1 \neq \beta_2$, or

$$t_0 = \frac{\Delta x^4 + \beta_1^4(\tau_1 - \tau_2)^2 - 2\beta_1^2\Delta x^2(\tau_1 + \tau_2)}{4\beta_1^2\Delta x^2}$$

otherwise.

After intersection, each crown has a circular part of radius R_{B1} and R_{B2} and the common curve defined as $\boldsymbol{x} = \boldsymbol{X}_B$. Denote (X_i, Y_i) the coordinates of the point of the intersection of the circular parts of the crowns at the time instant $t_i > t_0$ (see also the definition of the point $\boldsymbol{X}_i$ in figure 10 in § 5). These coordinates can be found from the geometrical conditions

$$X_i^2 + Y_i^2 = R_{B1}^2, \tag{4.10a}$$

$$(\Delta x - X_i)^2 + Y_i^2 = R_{B2}^2. \tag{4.10b}$$

The solution of the system (4.10) is

$$X_i(t_i) = \frac{R_{B1}^2(t_i) - R_{B2}^2(t_i) + \Delta x^2}{2\Delta x}, \tag{4.11a}$$

$$Y_i(t_i) = \sqrt{R_{B1}^2(t_i) - X_i^2(t_i)}. \tag{4.11b}$$

At time $t > t_i$ the material point located at the time instant t_i at (X_i, Y_i) belongs to the interface between two crowns. Equation (2.14) solved with the help of (4.8) subject to the initial conditions

$$t = t_i: \quad \boldsymbol{X}_B(t, t_i) = \boldsymbol{X}_i(t_i)$$

yields the following expression for the shape $\boldsymbol{X}_B(t, t_i)$ of the interface given in parametric form:

$$Y_B(t, t_i) = \frac{\sqrt{t + \tau_1}\sqrt{t + \tau_2}}{\sqrt{t_i + \tau_1}\sqrt{t_i + \tau_2}}\ Y_i(t_i), \tag{4.12a}$$

and

$$X_B(t,t_i)=\sqrt{t+\tau_1}\sqrt{t+\tau_2}\ \left[\frac{X_i(t_i)}{\sqrt{t_i+\tau_1}\sqrt{t_i+\tau_2}}+\frac{\Delta x}{\tau_1-\tau_2}\left(\frac{\sqrt{t+\tau_1}}{\sqrt{t+\tau_2}}-\frac{\sqrt{t_i+\tau_1}}{\sqrt{t_i+\tau_2}}\right)\right] \tag{4.12b}$$

with the parameter $t_i \in [t_0,\ t]$.

In the case $\tau_1 = \tau_2$ the solution of (2.14) takes the form

$$\boldsymbol{X}_B=\left(X_i(t_i)\frac{t+\tau_1}{t_i+\tau_1}-\frac{\Delta x}{2}\ \frac{t-t_i}{t_i+\tau_1}\right)\boldsymbol{e}_x+Y_i(t_i)\frac{t+\tau_1}{t_i+\tau_1}\ \boldsymbol{e}_y. \tag{4.13}$$

Now the analytical expressions for the velocity $\boldsymbol{V}_B$ of the upward jet at the interface $\boldsymbol{X}_B$, and the shape $\boldsymbol{X}_J$ of the jet can be determined by substituting (4.8) and (4.12) or (4.13) in (2.35) and (2.37), respectively.

5. Results and discussion

As in the model of Yarin & Weiss (1995) we also consider the initial phase of drop deformation when it becomes a disc of radius R_0 and thickness h_f. The duration of this first period is of order $t \approx 1$. Neglecting the momentum loss of the liquid during the drop deformation, invoking the mass balance of the drop, and considering the initial conditions at $t = 1$ yields the following expressions for the parameters of the problem:

$$\beta=\left(\frac{3h_f}{2}\right)^{-1/4},\quad \tau=\frac{1}{\sqrt{24h_f}}-1,\quad \eta=\frac{1}{24} \tag{5.1}$$

(h_f being the dimensionless initial thickness of the film).

The results of computations of the dimensionless height of the rim, $Z_R = \boldsymbol{X}_R(t)\cdot\boldsymbol{e}_z$, are shown in figure 5 for four different Weber numbers. The dimensionless film thickness is $h_f = 0.29$. The results of theoretical predictions are compared with experimental data from . The agreement is quite good.

The analytical shapes of the crown are shown in figure 6 at different time instants. The median surface of the crown $\boldsymbol{X}_J$, is defined by (3.2). The outer and inner surfaces of the crown are at distances $\pm h_J/2$ from the median surface, where the local jet thickness h_J is defined in (3.3). These two surfaces are reconstructed beginning from the point corresponding to $\boldsymbol{X}_J = \boldsymbol{X}_B$, $z = 0$. The smooth connection of these inner and outer surfaces of the crown with the free surface of the film on the wall are not considered in the present work. The predicted shape of the crown is nearly cylindrical, similar to the crowns observed in Cossali *et al.* (1997) or shown in figure 1.

Note that this shape is obtained by neglecting surface tension and viscosity effects. However, the resulting forces applied to the element of the surface of a free film associated with surface tension are directed normal to the film. Considering the near-cylindrical shape of the crown, the curvature of the crown is of order $\kappa \sim 1/R_B$. The thickness of the crown is of order $h_J \sim h_f$. Therefore, the term on the right-hand side of the momentum equation associated with the surface tension and neglected in equation (2.25) can be estimated in dimensionless form as $2\,(h_f We\, R_B)^{-1}$. Therefore the deviation ΔR_B of the crown radius due to surface tension can be estimated as $\Delta R_B \sim 2\,(h_f\, We\, R_B)^{-1}\,\Delta t$ where Δt is the time that a material point spends in the crown. This time is estimated as the ratio of the crown height to the vertical component of the jet velocity determined in (2.35). Using equations (1.1) and (5.1)

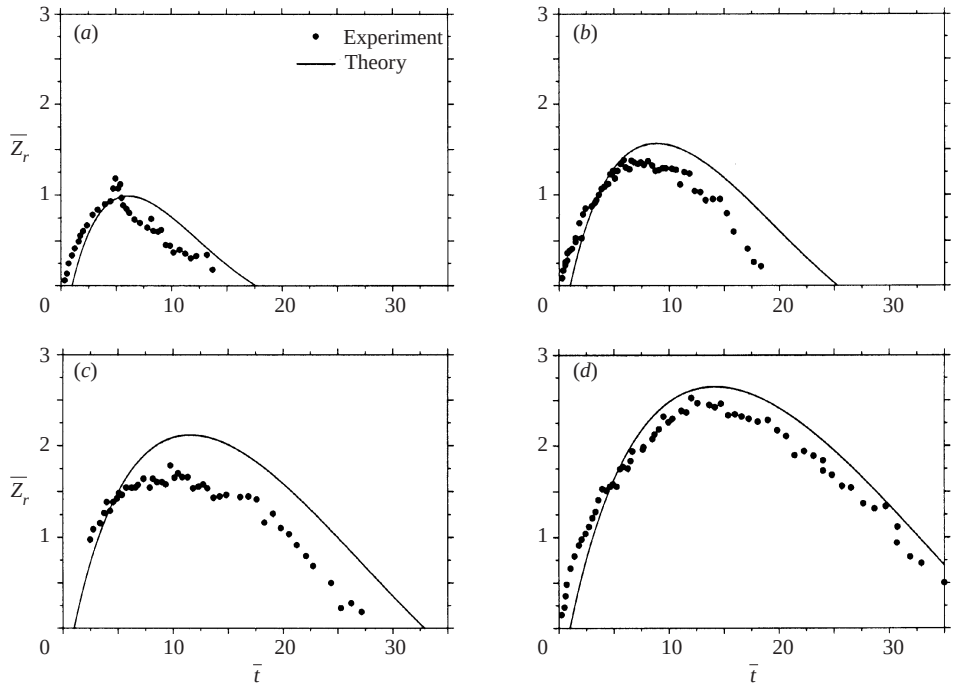

FIGURE 5. The height of the crown. Comparison of the theory with the experimental data Cossali *et al.* (1999), $\bar{h}_f = 0.29$: (*a*) $We = 297$, (*b*) $We = 484$, (*c*) $We = 667$, (*d*) $We = 842$.

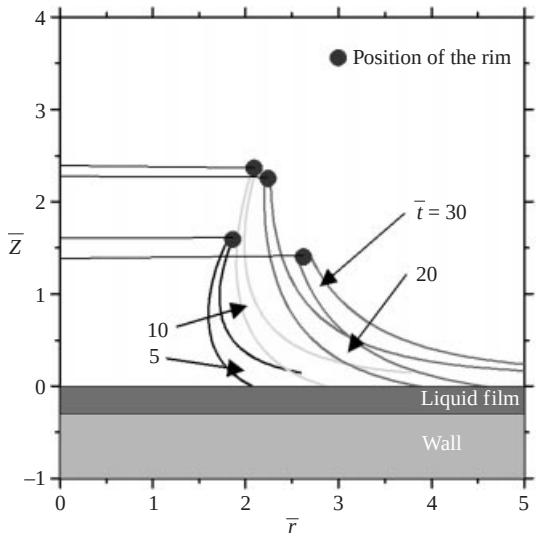

FIGURE 6. Predicted shape of the crown at different instants after drop impact. $\bar{h}_f = 0.29$, $We = 842$, $Fr^{-1} = 0$. Time instants are: $\bar{t} = 5$, 10, 20 and 30.

leads to

$$\frac{\Delta R_B}{R_B} \sim \frac{Z_r^2}{We}.$$

Note also that the formation of the crown and splash takes place in the case of high Weber number, when the surface tension effect is small. Specifically, in the cases

shown in figure 5, the Weber numbers range from 297 to 842, whereas the height of the crown is of order $Z_r \sim 1$. Therefore, the error $\Delta R_B/R_B$ due to surface tension in the cases considered is negligibly small.

The shape (3.2) of the crown is obtained using an assumption of a simple ballistic trajectory for liquid particles – the same principle used in Peregrine (1981). However, the present results are very different from those obtained in Peregrine (1981). The first main difference is in the use of the square-root time dependence (1.1) of the radius R_B and not a linear dependence as predicted in Peregrine (1981). Second, the prediction of the thickness of the crown is added, which allows a description of the propagation of the rim at the edge of the crown.

The shape of the base of the crown in the case of oblique impact at long times $t \gg 1$ is predicted in (4.3). This shape is an ellipse with constant ratio of the half-axes γ. We can only speculate about the value of γ in the absence of experimental data. However, extrapolating the assumption of constant γ also into the time interval $t < 1$ and noting that the initial shape of the drop is spherical and thus the initial spot which is created on the wall is circular, we conclude that the value of γ must be close to unity. Therefore, $\beta_x \approx \beta_y = \beta$, and the shape of the kinematic discontinuity is a circle of radius $\beta\sqrt{t+\tau}$.

The initial displacement x_0 of the centre of the circle at the instant $t \approx 1$ is assumed to be small and is neglected. This assumption together with the assumed circular shape of the initial spot means that the influence of the outer flow $\boldsymbol{V}_\tau$ on the film during the short first phase ($t < 1$) of the impact is assumed to be negligibly small. Therefore, the parameters β, τ and η are the same as in the normal impact of a single drop and are determined in (5.1).

It is more convenient to present the results on oblique impact in the coordinate system moving with the outer film with the velocity $-V_\tau \boldsymbol{e}_x$. This coordinate system corresponds to the oblique impact of a drop with the initial tangential velocity $V_\tau \boldsymbol{e}_x$ onto a steady uniform film of the thickness h_f. Following (4.3) and (5.1) the x-coordinate x_c of the centre of the circle and its radius R_B are

$$x_c = V_\tau\,(\sqrt{1+\tau}\,\sqrt{t+\tau} - \tau), \quad R_B = \left(\frac{3h_f}{2}\right)^{-1/4}\sqrt{t+\tau},$$

and the angle φ^* defined in (4.6) becomes

$$\varphi^* = \arccos(-2/V_\tau).$$

Therefore, the minimal obliquity angle θ^* between the drop velocity vector and the normal to the wall, at which the base of the crown is no longer a closed circle, can be estimated as $\theta^* = \arctan(2) \approx 63.4^\circ$.

The predicted shapes of the base of the crown are shown in figure 7 for three different values of the dimensionless tangential velocity V_τ of the drop. The base of the crown is shown only at points where the source term Q defined in (4.5) is positive, meaning that at these points an inclined jet is produced. It is shown that if the impact angle θ is not zero ($\theta = \pi/4$ on figure 7*b*), the shape of the crown can be represented as a moving, expanding circle. If the impact angle is smaller than some critical value ($\theta = \arctan(3) \approx 1.249$ in figure 7*c*), the shape of the base of the crown is no longer a closed curve. A similar behaviour of the crown after an oblique drop impact was observed in the experimental study of Lavergne & Platet (2000). The shapes of the crowns predicted using (4.3) and (4.7) in (2.37) are shown in figures 8 and 9 for two different obliquity angles: $\theta = \pi/4 < \theta^*$ (figure 8), and $\theta = \arctan(3) > \theta^*$ (figure 9).

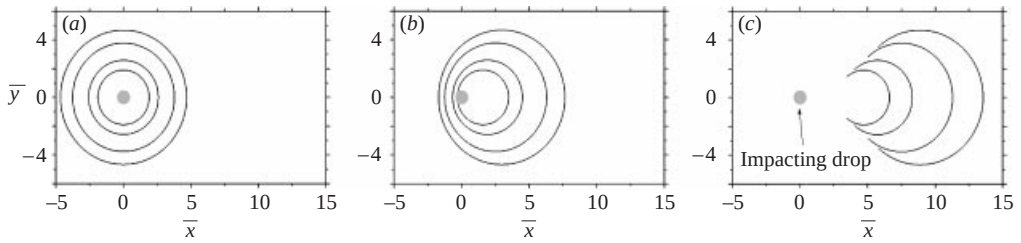

FIGURE 7. Shape of the base of the crown in the case of an oblique impact at time instants: $\bar{t} = 5$, 10, 15. The dimensionless thickness of the film is $\bar{h}_f = 0.29$. (*a*) Normal impact, $\overline{V}_\tau = 0$, (*b*) $\overline{V}_\tau = 1$, (*c*) $\overline{V}_\tau = 2$.

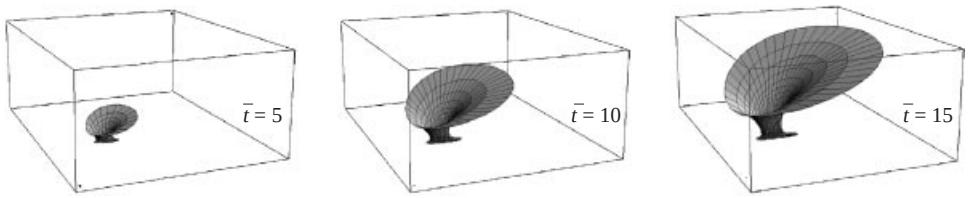

FIGURE 8. Shape of the crown produced due to an oblique impact. $\bar{h}_f = 0.29$, $\overline{V}_\tau = 1$, $We \to \infty$.

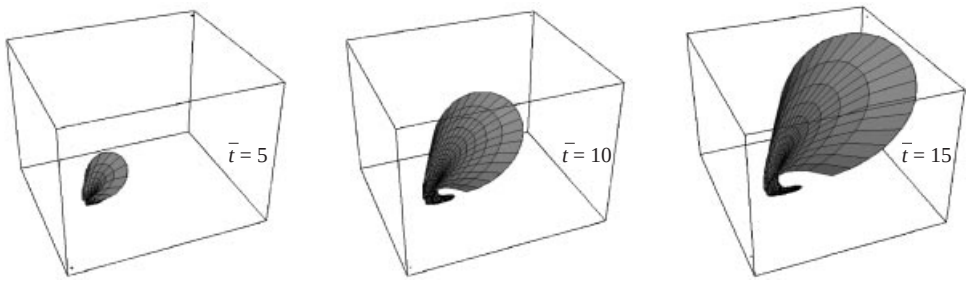

FIGURE 9. Shape of the crown produced due to an oblique impact. $\bar{h}_f = 0.29$, $\overline{V}_\tau = 3$, $We \to \infty$.

In the case of the impact of two drops of diameters D_1 and D_2 with impact velocities U_1 and U_2, the parameters β_1, τ_1 and η_1 are determined in (5.1). The parameters β_2, τ_2 and η_2 can be obtained using (5.1) in (4.9) in the form

$$\beta_2 = k_u^{1/2}\, k_d^{3/4} \left(\frac{3h_f}{2}\right)^{-1/4}, \quad \tau_2 = \frac{k_u}{k_d}\left(\frac{k_d}{\sqrt{24h_f}} - 1\right) - \Delta t, \quad \eta_2 = \frac{k_d^3}{24\, k_u}$$

(h_f being the non-dimensional film thickness with the diameter D_1 used as a length scale).

The results of the theoretical predictions of the shape of the interface between two crowns on the wall are shown in figures 10–12 at different times t after impact. It should be noted that in the expression for the curve $\boldsymbol{X}_B$ determined in (4.12) or (4.13) and corresponding to this interface, the component of the velocity parallel to the curve t is not considered. This component does not influence the shape of the curve. However, in some cases it can lead to the extension of the theoretical line beyond the space occupied by the crowns on the wall, which has no physical sense.

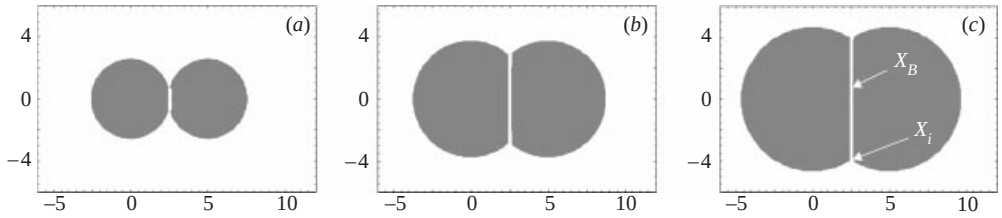

FIGURE 10. Symmetric interaction of two drops. $\bar{h}_f = 0.29$, $\Delta\bar{x} = 5$, $\Delta\bar{t} = 0$, $k_d = 1$, $k_u = 1$. The non-dimensional times $\bar{t}$ after impact are: (*a*) 5, (*b*) 10, and (*c*) 15.

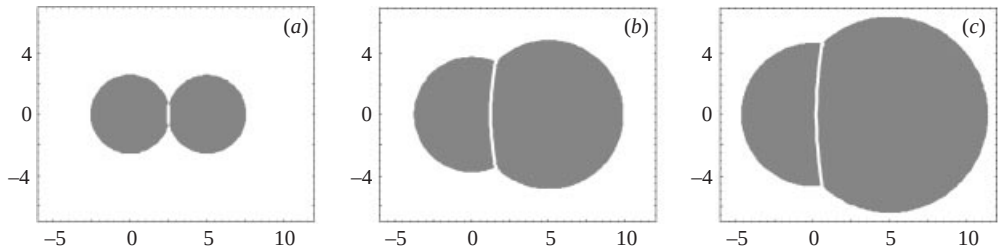

FIGURE 11. Interaction of two drops of the same diameter and different impact velocity impacting simultaneously. $\bar{h}_f = 0.29$, $\Delta\bar{x} = 5$, $\Delta\bar{t} = 0$, $k_d = 1$, $k_u = 3$. The non-dimensional times $\bar{t}$ after impact are: (*a*) 5, (*b*) 10, and (*c*) 15.

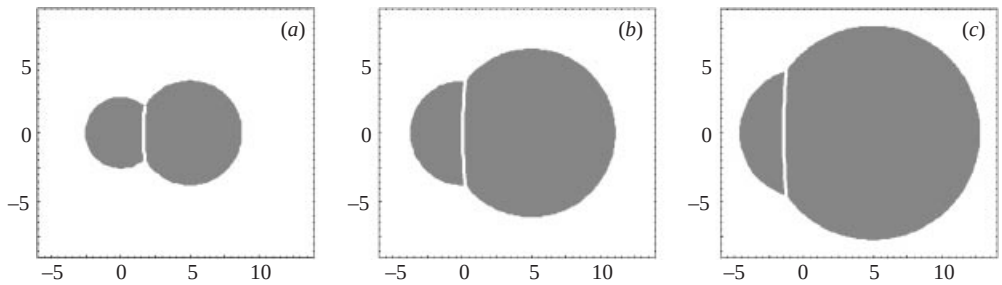

FIGURE 12. Interaction of two drops of different diameter and impact velocity. $\bar{h}_f = 0.29$, $\Delta\bar{x} = 5$, $\Delta\bar{t} = 3$, $k_d = 2$, $k_u = 0.8$. The non-dimensional times $\bar{t}$ after impact are: 5, 10, and 15.

In figures 10–12 only the part of the curve $\boldsymbol{X}_B$ is shown which belongs to the discs of radii R_{B1} and R_{B2}.

In figure 10 the symmetric case is shown, when two drops of the same diameter and the same impact velocity impact onto the film simultaneously. The grey discs correspond to the inner fields of two crowns, and the white line is the interface between these crowns. Due to symmetry, the interface $\boldsymbol{X}_B$ is a straight line coinciding with the symmetry axis.

The non-symmetric case, when the second drop has the same diameter as the first one but a higher impact velocity, is shown in figure 11; this illustrates the simultaneous impact of two drops. In figure 12 the case of the interaction of two crowns produced by impacting drops of different initial diameters and impact velocities is shown. The time interval between these two impacts is not zero.

6. Conclusions

The equations for the shape of the kinematic discontinuities and for the velocity vector and the thickness of the jet formed at this kinematic discontinuity are developed for the general case of drop impact on wetted surface. The model for the crown shape takes into account inertial effects and neglects surface tension and viscous forces in the crown. Surface tension effects are accounted for in the description of the motion of the free rim bounding the crown. The model is valid for the high-velocity impact of a low viscosity liquid drop on a relatively thin liquid film. The theoretical prediction for the height of the crown is compared with experimental data in the literature. The results of the comparison are good, in spite of the fact that no adjustable parameters are used. Some results for the shape of the base of the crown in the case of oblique impact and interaction of two crowns are presented.

This research was partially supported by GIF – German–Israeli Foundation for Scientific Research and Development, Research Grant No. I-536-097.14/97.

REFERENCES

Böhm, C., Weiss, D. A. & Tropea, C. 1999 Multi-droplet impact onto solid walls: droplet–droplet interaction and collision of kinematic discontinuities. In *Proc. 15th Ann. Conf. on Liquid Atomization and Spray Systems, Darmstadt* (ed. C. Tropea & K. Heukelbach), pp. VII.7.1–VII.7.6.

Cossali, G. E., Brunello, G., Coghe, A. & Marengo, M. 1999 Impact of a single drop on a liquid film: experimental analysis and comparison with empirical models. *Proc. Italian Congress of Thermofluid Dynamics UIT, Ferrara, Italy*.

Cossali, G. E., Coghe, A. & Marengo, M. 1997 The impact of a single drop on a wetted surface. *Exps. Fluids* **22**, 463–472.

Harlow, H. & Shannon, J. P. 1967 The splash of a liquid drop. *J. Appl. Phys.* **38**, 3855–3866.

Lavergne, G. & Platet, B. 1999 Droplet impingement on cold and wet wall. *Proc. 15th Ann. Conf. on Liquid Atomization and Spray Systems, Darmstadt* (ed. C. Tropea & K. Heukelbach), pp. VII.12.1–VII.12.6.

Levin, Z. & Hobbs, P. V. 1971 Splashing of water drops on solid and wetted surfaces: hydrodynamics and charge separation. *Phil. Trans. R. Soc. Lond.* A **269**, 555–585.

Macklin, W. C. & Metaxas, G. J. 1976 Splashing of drops on liquid layers. *J. Appl. Phys.* **47**, 3963–3970.

Mundo, C., Sommerfeld, M. & Tropea, C. 1994 Experimental studies of the deposition and splashing of small liquid droplets impinging on a flat surface. In *Proc. 6th Intl Conf. on Liquid Atomization and Spray Systems* (ed. A. J. Yule & C. Dumouchel), pp. 134–141. Rouen.

Mundo, C., Sommerfeld, M. & Tropea, C. 1998 On the modelling of liquid sprays impinging on surfaces. *Atomization and Sprays* **8**, 625–652.

Peregrine, D. H. 1981 The fascination of fluid mechanics. *J. Fluid Mech.* **106**, 59–80.

Prosperetti, A. & Oguz, H. N. 1993 The impact of drops on liquid surfaces and the underwater noise of rain. *Anu. Rev. Fluid Mech.* **25**, 577–602.

Rein, M. 1993 Phenomena of liquid drop impact on solid and liquid surfaces. *Fluid Dyn. Res.* **12**, 61–93.

Rieber, M. & Frohn, A. 1999 A numerical study on the mechanism of splashing. *Intl J. Heat Fluid Flow* **20**, 455–461.

Roisman, I. V., Araneo, L., Marengo, M. & Tropea, C. 1999 Evaluation of drop impingement models: experimental and numerical analysis of a spray impact. In *Proc. 15th Ann. Conf. on Liquid Atomization and Spray Systems, Toulouse* (ed. G. Lavergne).

von, Schelkle, M., Rieber, M., Frohn, A. 1999 Numerische Simulation von Tropfenkollisionen. *Spektrum der Wissenschaft*, January, 72–79.

Shin, J. & McMahon, T. A. 1990 The tuning of a splash. *Phys. Fluids* A **2**, 1312–1317.

Taylor, G. I. 1959 The dynamics of thin sheets of fluid II. Waves on fluid sheets. *Proc. R. Soc. Lond.* A **263**, 296–312.

Tropea, C. & Roisman, I. V. 2000 Modelling of spray impact on solid surfaces. *Atomization and Sprays* **10**, 387–408.

Trujillo, M. F. & Lee, C. F. 2001 Modeling crown formation due to the splashing of a droplet. *Phys. Fluids* **13**, 2503–2516.

Walzel, P. 1980 Zerteilgrenze beim Tropfenaufprall. *Chem. Ing. Tech.* **52**, 338–339.

Wang, A.-B. & Chen, C.-C. 2000 Splashing impact of a single drop onto very thin liquid films. *Phys. Fluids* **12**, 2155–2158.

Weiss, D. A. & Yarin A. L. 1999 Single drop impact onto liquid films: neck distortion, jetting, tiny bubble entrainment, and crown formation. *J. Fluid Mech.* **385**, 229–254.

Whitham, G. B. 1974 *Linear and Nonlinear Waves*. Wiley.

Yarin, A. L. 1993 *Free Liquid Jets and Films: Hydrodynamics and Rheology*. Longman & Wiley.

Yarin, A. L. & Weiss D. A. 1995 Impact of drops on solid surfaces: self-similar capillary waves, and splashing as a new type of kinematic discontinuity. *J. Fluid Mech.* **283**, 141–173.